IOP Publishing Physica Scripta
Phys. Scr. 95 (2020) 065404 (7pp) https://doi.org/10.1088/1402-4896/ab802d

Excitation-autoionization contribution to single ionization of Sr by electron impact

V Borovik[1], I Shafranyosh[1] and O Borovik[1,2]

[1] Uzhgorod National University, Uzhgorod, 88000, Ukraine
[2] Institute of Electron Physics, Uzhgorod, 88017, Ukraine

E-mail: vladimir.borovik@uzhnu.edu.ua

Received 25 January 2020, revised 10 March 2020
Accepted for publication 16 March 2020
Published 18 May 2020

Abstract

The $4p^6$ excitation-autoionization (EA) cross-section of Sr atoms has been measured at electron-impact energies from the threshold to 600 eV. The cross-section has a pronounced resonance character in the near-threshold region, reaching its maximum value of $(2.5 \pm 0.8) \times 10^{-16}$ cm^2 at 24.5 eV. The shape and absolute value of the cross-section are determined by the excitation dynamics and the decay mode of autoionizing states from $4p^5 4d 5s^2$, $4p^5 4d^2 nl$ and $4p^5 4d 5s nl$ configurations. A comparative analysis of the measured EA cross-section, the calculated $5s^2$ ionization cross-section and the available ionization data showed that (i) direct ionization of the $5s^2$ shell and EA of the $4p^6$ shell adequately describe the single ionization of Sr atoms; (ii) $4p^6$ EA contribution reaches 25% of the total single ionization cross-section of Sr atoms.

Keywords: atom, single ionization, autoionization, cross-section

1. Introduction

The spectra of ejected electrons studied in a broad range of impact energies are the only source of data on the energy structure, excitation cross-sections, and decay channels of atomic and ionic autoionizing states. The lack of relevant theoretical data, especially at low impact energies, makes such information the only available basis for modern studies of many-electron atoms using ultrashort photon beams [1, 2].

Strontium has a widespread use in various fundamental physical [2–4] and technical [5–7] tasks. Meanwhile, as an atomic system, it is still poorly understood. Such fundamental characteristics as the structure of energy levels, the processes of excitation, ionization, and autoionization, are very little studied. For example, the available information on the level structure is limited to the $5s^2$ valence shell [8], and existing studies of the processes of excitation [9, 10] and ionization [11–14] differ greatly in the absolute values of corresponding cross-sections.

The autoionization processes in Sr atoms are associated with the excitation of the $5s^2$ and $4p^6$ shells. Highly excited levels $4p^6 n_1 l_1 n_2 l_2$ and $4p^5 n_1 l_1 n_2 l_2 n_3 l_3$ were observed in the photoabsorption spectra in the ranges of 174–200 nm [15, 16] and 30–80 nm [17–19], respectively. However, the nonradiative decay was studied mainly for the second group of levels [20–23]. In these and subsequent studies [24, 25] it was suggested that the sharp increase in the ionization cross-section observed at impact energies above 21 eV [11–14] is due to the following excitation-autoionization (EA) process

$$\mathrm{Sr}(4p^6 5s^2) + e_{\mathrm{inc}} \rightarrow \mathrm{Sr}^*(4p^5 n_1 l_1 n_2 l_2 n_3 l_3) + e_{\mathrm{sc}} \quad (1)$$

$$\hookrightarrow \mathrm{Sr}^{+*}(4p^6 nl) + e_{\mathrm{ej}} \quad (2)$$

The EA processes significantly increase the ionization cross-section and thereby affect the charge and temperature of various plasma media [26–28]. The first quantitative assessment of the role of autoionization in electron-impact ionization was experimentally made for alkali atoms (see [29] and references therein). Recently, similar data were obtained for Ba atoms [30]. The role of the $4p^6$ subshell in the ionization of Sr atoms was considered only theoretically. To explain their experimental data, Veinstein *et al* [14] used the Born and classical binary approximations. Roy and Rai [31] performed *ab initio* calculations using the binary encounter approximation with the symmetrical collision model of Vriens and a Hartree–Fock velocity distribution for the bound electron. In both calculations, the contribution from the excitation of the $4p^6$ subshell was taken into account. The results obtained describe the behavior of the

experimental ionization cross-section [12–14] only in general terms, giving a markedly overestimated contribution from the $4p^6$ subshell. The role of the $4p^6n_1l_1n_2l_2$ states in the ionization of Sr atoms has not yet been considered.

The absolute value of the autoionization contribution of a particular electron shell to the ionization cross-section is described by the cross-section of the corresponding EA process [32] and can be defined as

$$\sigma_{EA}|_E = \sum_{j,f} \sigma_{exc}(j)|_E \, B(j \to f), \tag{3}$$

where $\sigma_{exc}(j)|_E$ is the excitation cross-section of the autoionizing state j at impact-energy value E and $B(j \to f)$ is the branching ratio for the decay of this state to the final state f of an ion

$$B(j \to f) = \frac{A^a(j \to f)}{\sum_f A^a(j \to f) + \sum_i A^r(j \to i)}, \tag{4}$$

where $A^r(j \to i)$ is the probability of radiative decay of the state j to the lower level i of an atom.

As shown in the studies of alkali atoms [29], accurate measurements of the intensity of the energy spectra of ejected electrons e_{ej} in a broad impact-energy range make it possible to obtain the energy dependence and the absolute value of the σ_{EA} cross-section with acceptable accuracy. Indeed, the excitation cross-section $\sigma_{exc}(j)|_E$ in (3) is related to the intensity $I(j \to f)|_E$ of the ejected-electron line arising from the radiationless decay of the autoionizing state j with formation of the ion in a state f as

$$I(j \to f)|_E \sim \frac{\sigma_{exc}(j)|_E}{4\pi} B(j \to f) C_K, \tag{5}$$

where C_K is the asymmetry parameter characterizing the angular distribution of ejected electrons [33].

If the spectroscopic identification of lines in ejected-electron spectra is known, all decay channels of corresponding autoionizing states are known too. In this case, the cross section $\sigma_{exc}(j)|_E$ and, therefore, the EA cross-section $\sigma_{EA}|_E$ can be determined experimentally as the sum of normalized intensities $I(j \to f)|_E$ of the lines reflecting all decay channels of the state j in the ejected-electron spectrum measured at the impact-energy value E.

Recently, we have studied the ejected-electron spectra of Sr atoms in an impact energy range from the $4p^6$ excitation threshold up to 102 eV and identified 60 lines with multichannel decay of 105 autoionizing states in the $4p^55s^2nl$, $4p^54d^2nl$ and $4p^55snln'l'$ configurations [25]. In the present work, we have extended this study up to 600 eV electron-impact energy and obtained the absolute value and the energy dependence of the EA cross-section for the $4p^6$ subshell. Based on the spectroscopic classification and excitation dynamics of the $4p^5n_1l_1n_2l_2n_3l_3$ states, the role of particular electron configurations in formation of the EA cross-section was considered. In order to evaluate the relative contribution of the autoionization to the total single ionization cross-section of Sr atoms, the experimental results, supplemented by calculations of the excitation and ionization cross-sections for the $5s^2$ shell were compared with the available experimental and theoretical data.

The paper is organized as follows. In section 2, we briefly describe the employed experimental and theoretical methods. In section 3, the measured and calculated results are considered and discussed together with other available data. Conclusions are drawn in section 4.

2. Measurement and calculation technique

Experiment. The measurements were carried out on a electron-atom collision setup, which has been previously employed in a number of studies of the electron spectra of metal vapors [34, 35]. In the present study, two different sources of incident electrons have been employed: an electrostatic 127° monochromator with the energy resolution of 0.2 eV (FWHM) was used for the near-threshold energy region and a five-electrode electron gun with the energy spread of the beam $\leqslant$0.5 eV (FWHM) was used at the energies beyond 50 eV [36].

The ejected-electron spectra corresponding to the electron decay of the $4p^5n_1l_1n_2l_2n_3l_3$ states were measured for the incident-electron energy values from the excitation threshold of the $4p^6$ shell at 20.98 eV [25] up to 600 eV using various increment steps with the shortest one being 0.1 eV. The ejected-electron energy analyzer (a 127° cylindrical deflector) was positioned at a 'magic' angle of 54.7° to minimize the possible influence of the asymmetry of the angular distribution of ejected electrons on the impact-energy dependence of the line intensity in the measured spectra [33]. Examples of spectra at impact energies of 30.7 and 600 eV are shown in figure 1.

In accordance with the method described in section 1 (see equations (3)–(5)), the EA cross-section $\sigma_{EA}(4p^6)$ at a given impact energy value E was determined as the sum of the normalized intensities of the lines observed in the ejected-electron spectrum measured at this energy. The final value of the cross-section was obtained as the average value from three independent measurements. The total relative uncertainty does not exceed 35% for impact energies below 30 eV and 30% for higher energies. The main source of uncertainty was the procedure for subtracting the continuous background from the original spectrum. The obtained EA cross-section in relative units was normalized at 600 eV impact energy to the calculated excitation cross-section of the $4p^54d(^1D)5s(^2D)6s\ ^3D_1$ state (see line 76 in the spectra in figure 1).

Calculations. In the case of independent processes (ionization and autoionization), the total single ionization cross-section $\sigma^+_{tot}(nl)$ of an electron subshell nl (partial cross-section) can be written as

$$\sigma^+_{tot}(nl) = \sigma^+_{dir}(nl) + \sigma_{EA}(nl), \tag{6}$$

where $\sigma^+_{dir}(nl)$ and $\sigma_{EA}(nl)$ are cross sections for direct ionization and EA process, respectively, and

$$\sigma^+_{dir}(nl) = \sum_f \sigma^+_{dir}(f). \tag{7}$$

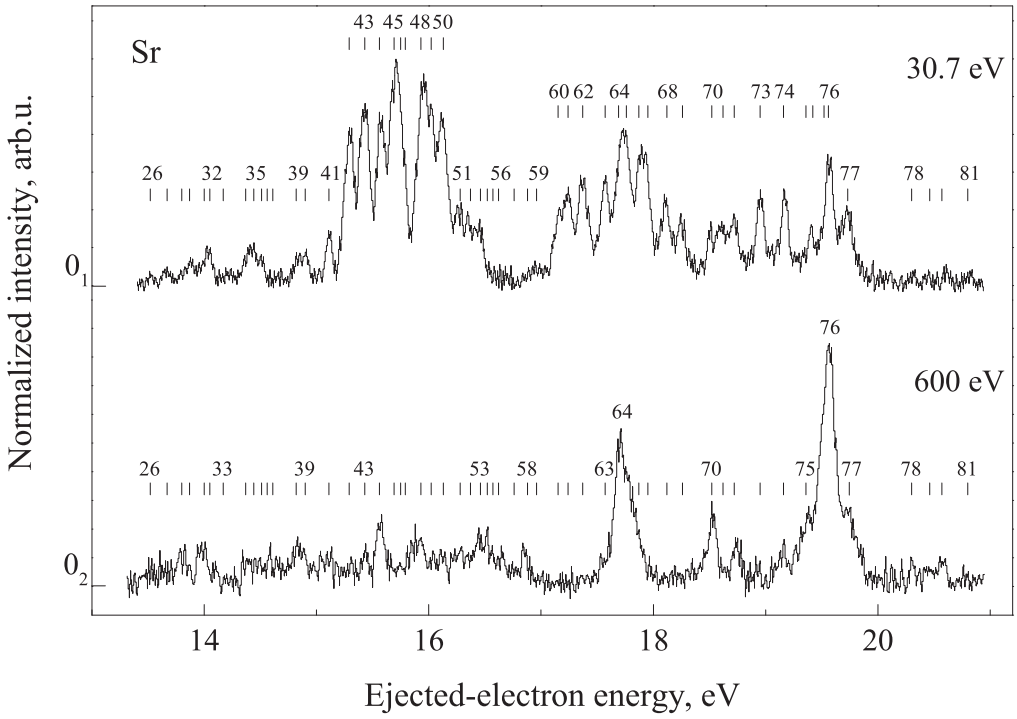

Figure 1. The ejected-electron spectra of Sr atoms at 30.7 and 600 eV incident-electron energies. In spectra, a polynomial background function was subtracted from the original data. Bars on top of the spectra mark the positions of ejected-electron lines. The indexation of lines is according to [21].

In (7), $\sigma^{+}_{dir}(f)$ is the ionization cross-section of an atom with formation of an ion in a final state f. According to the energy conservation rule, the summation in (7) includes all the states of an ion that can be reached at impact energy E.

In previous studies electron-impact single ionization of Sr atoms was theoretically considered in the binary-encounter (BE) approximation with classical (C-BE) [14] and symmetrical (S-BE) [31] approaches. However, the Sr atom is a many-electron system for which relativistic and correlation effects must play an important role, even if we consider the outer valence shell. To take these effects into account, the cross-section $\sigma^{+}_{dir}(5s^2)$ was calculated in the relativistic distorted wave (RDW) [25] approximation using single- (SC) and multiconfiguration (MC) approaches. To demonstrate the role of relativism and correlations in the description of Sr ionization, we also used for calculations the binary-encounter-dipole (BED) [37] approximation in SC and MC approaches, and the empirical formula by Lotz (EF-Lotz) [38]. In the RDW and BED approximations, the same basis set was used to calculate ionization and excitation cross-sections. In both approximations, the radial wave functions were obtained as numerical solutions of the Dirac-Fock-Slater equations [39]. Excitation cross-sections were obtained in the RDW approximation using a calculation procedure similar to that described in detail elsewhere [25, 40].

3. Results and discussion

EA cross-section. In figure 2, the measured EA cross-section $\sigma_{EA}(4p^6)$ is shown in the range of impact energies 15–600 eV. At low impact energies, the cross-section possesses a pronounced resonance character with a 'fine' structure *a*, *b* and *c* at 22.5, 24.5 and 26.8 eV, respectively (see also the inset). The cross-section reaches the maximum value of $(2.5 \pm 0.8) \times 10^{-16}\,\mathrm{cm}^2$ at 24.5 eV impact energy (maximum *b*). Above 50 eV, the cross-section increases slowly, forming a broad maximum around 100 eV. With further increase in impact energy, the cross-section decreases monotonically to the value of $(0.3 \pm 0.1) \times 10^{-16}\,\mathrm{cm}^2$ at 600 eV.

In accordance with definitions (3)–(5), the measured cross-section as a whole is the resulting excitation function of the entire set of autoionizing states observed in the ejected-electron spectra. Consequently, its impact-energy behavior should reflect the peculiarities of excitation dynamics of individual states or their groups. Indeed, as can be seen in figure 2, the fast rise of the cross-section just above the $4p^6$ excitation threshold reflects the strong resonance excitation of the group of three lowest autoionizing states $4p^5 4d 5s^2\ {}^3P_1$, ${}^3P_2$ and ${}^3F_4$ [24]. The maximum *a* as a whole reflects the near-threshold excitation dynamics of the states $4p^5 4d 5s^2$ with excitation thresholds between 21 and 23 eV (see lines 42–45, 48–50, 52, 53 in figure 1 and table 2 in [25]). Similarly, maxima *b* and *c* reflect the resonance excitation of two groups of the states from $4p^5 4d 5s^2$, $4p^5 4d^2 5s$, 5p, $4p^5 4d 5s 6s$, 5d, 7s (lines 62–74) and $4p^5 4d 5s 6d,7d$ (lines 75–81) configurations lying between 23–25 eV and 26–28 eV, respectively. A fast decrease in the cross-section observed above 27 eV is associated with the absence in ejected-electron spectra of the lines reflecting the decay of autoionizing states with such high excitation thresholds. This is due to the opening of a new decay channel for such states, namely, decay into ionic autoionizing states $4p^5 n_1 l_1 n_2 l_2$

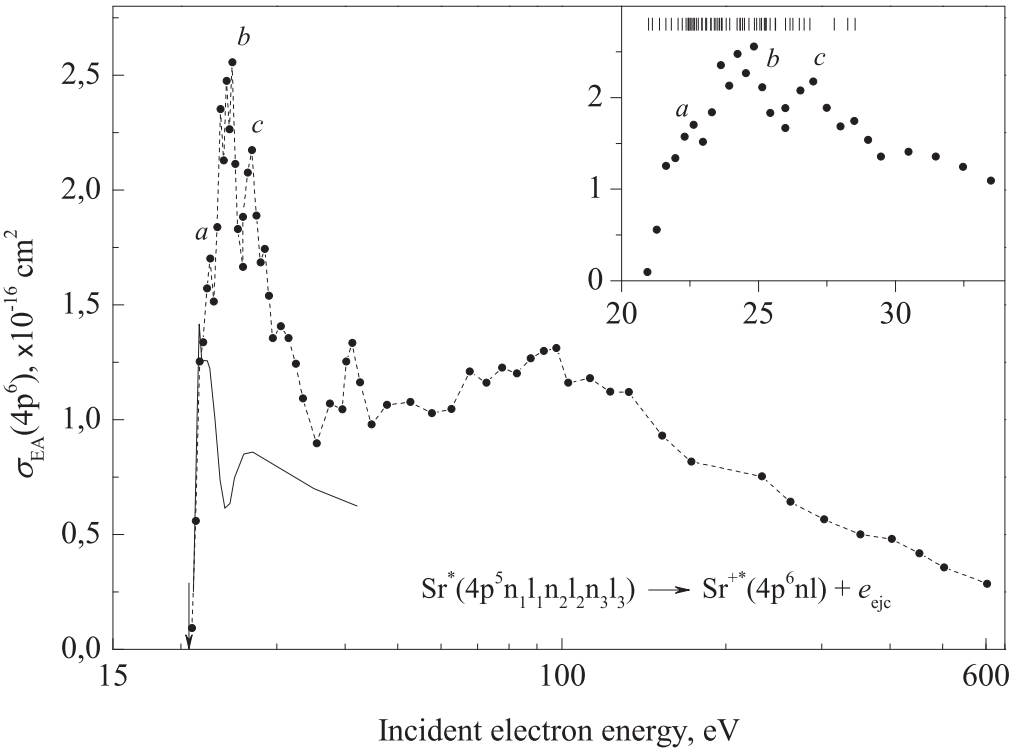

Figure 2. EA cross-section $\sigma_{EA}(4p^6)$ of Sr atoms. Solid line represents the sum of excitation cross-sections of the states $4p^54d5s^2\ ^3P_1$, $^3P_2$ and $^3F_4$ [24]. Vertical arrow marks the $4p^6$ excitation threshold at 20.98 eV. Inset shows the low-energy part of the $\sigma_{EA}(4p^6)$ cross-section (see text); bars on top mark the position of the $4p^5n_1l_1n_2l_2n_3l_3$ autoionizing states [25].

with excitation thresholds above 26.9 eV [41]. This decay process is known as the first step of two-step autoionization [42] which leads to the formation of Sr^{2+} ions in the ground state $4p^6\ ^1S_0$ [25]. At the impact energies beyond 40 eV, the behavior of the cross-section $\sigma_{EA}(4p^6)$ is determined by the excitation dynamics of dipole-allowed states ($\Delta J = 1$) mainly from $4p^54d5s^2$ and $4p^54d^25s$ configurations lying above 25 eV (lines 63–77).

Ionization and autoionization. In Sr atoms, the total single ionization cross-section σ^+_{tot} can be represented by the sum of partial cross-sections $\sigma^+_{tot}(nl)$, $nl = 5s^2$, $4p^6$, $4s^2$, $3d^{10}$ and other deeper subshells. Theoretical estimates made in this work and those in [14], as well as a comparison with ionization data for Rb atoms [40] show that the maximum contribution from ionization and excitation-autoionization of the $4s^2$ and $3d^{10}$ subshells can be no more than 3%–4%.

The direct ionization of the $4p^6$ subshell in Sr leads to the formation of the $4p^5n_1l_1n_2l_2$ ionic states with the excitation thresholds above 26.9 eV [21, 41]. All these states effectively autoionize into the $4p^6\ ^1S_0$ ground state of Sr^{2+} [43]. Thus, the direct ionization of the $4p^6$ subshell contributes exclusively to the double ionization process and should be excluded from the present consideration.

Figure 3 shows the currently available experimental data on the total single ionization cross-section σ^+_{tot} [12] and the total ionization cross-section $\sigma_{ion} = \sigma^+_{tot} + \sigma^{2+}_{tot} + \sigma^{3+}_{tot} + ...$ [13, 14] of Sr atoms. Note that the latter cross-section also represents the σ^+_{tot} cross section at impact energies below the threshold for two-step autoionization at 26.9 eV. As can be seen, although the experimental cross-sections differ in absolute value, they are similar in shape in the impact-energy region up to the threshold for two-step autoionization.

Considering the calculated cross-sections presented in figure 3, it is easy to see that they all differ from each other in both the value and the position of the maxima. The RDW cross-sections are shifted closer to the ionization threshold, and the maxima of the BED, EF-Lotz and C-BE cross-sections are closer to the experimental data. Taking into account the configuration interaction noticeably reduces the RDW and BED cross-sections, bringing them closer to the experimental values [13, 14] but shifting the RDW-MC cross-section even closer to the ionization threshold. Given the shape and absolute value of the calculated cross-sections as well as taking into account the possible contribution from doubly-excited states, one may say that the ionization cross-section BED-MC provides the best agreement with the experimental data [13, 14]. This conclusion is also supported by our earlier analysis of the single ionization cross-section of Rb atoms [40].

For a comparative analysis of the cross-sections with remarkably different absolute values, it is convenient to represent them in relative units. For this, the calculated cross-sections were normalized to their maximum values, and the experimental data [12–14] were normalized to their values at 17.3 eV impact energy (see the inset in figure 3). As can be seen, the experimental data [12, 14] practically coincide in behavior up to the threshold for two-step autoionization. At impact energies above 21 eV, the data [13] underestimate the $4p^6$ EA contribution.

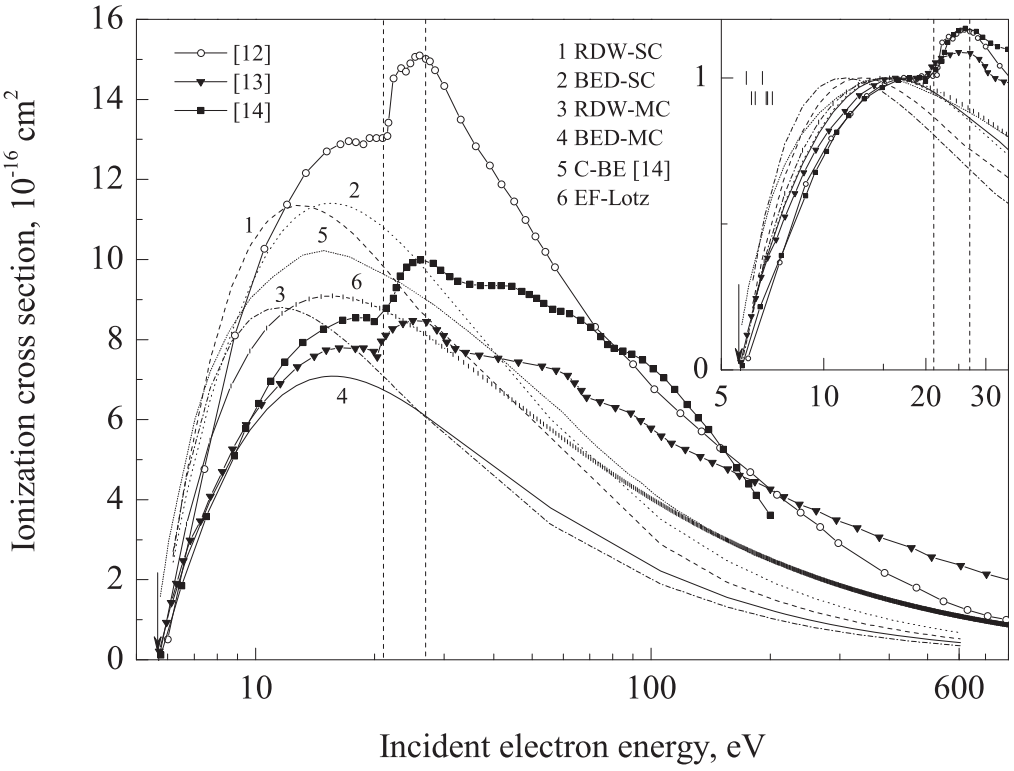

Figure 3. The present RDW, BED, EF-Lotz and C-BE [14] calculated $5s^2$ ionization cross-sections compared with experimental ionization cross-sections of Sr atoms by electron impact [12–14]. Arrow marks the $5s^2$ ionization threshold at 5.69 eV while the vertical dashed lines mark the excitation threshold of the $4p^6$ subshell at 20.98 eV[25] and the threshold for two-step autoionization at 26.9 eV [21, 41]. Inset shows the cross-sections in relative units (see text) and positions of the most intensive broad lines in photoabsorption spectra [15] (bars in bottom row) and in electron energy-loss spectra [25] (bars in top row).

As mentioned in Introduction, the simultaneous excitation of two valence 5s electrons leads to the formation in Sr of the $4p^6 n_1 l_1 n_2 l_2$ autoionizing states (see bars in the inset in figure 3). An analysis of the experimental ionization curves [12–14] between the ionization threshold at 5.69 eV and 15 eV does not reveal any clear thresholds that may indicate the EA contribution of these states. However, it would be premature to consider that the contribution from $5s^2$ shell is negligible. A shift of the first maxima in the experimental ionization cross-sections relative to the maxima of the calculated cross-sections towards higher energies can be the result of this contribution. Our estimates of the $5s^2$ EA cross-section within the RDW-CI approximation give a value of 2.5×10^{-16} cm^2 at 20 eV, which is probably overestimated due to the weakness of such calculations at low impact energies. Comparison of the absolute values of our calculated cross-section BED-MC and the experimental cross sections [13, 14] at 20 eV gives the value of the $5s^2$ EA cross-section in the range $(0.8–1.6) \times 10^{-16}$cm^2 which is within the systematic error of 10%–15% of the experimental data [13, 14]. For a final conclusion regarding the role of the $5s^2$ shell in the ionization of Sr atoms, we have added the calculated cross-section BED-MC $\sigma_{dir}(5s^2)$) to the measured EA cross-section $\sigma_{EA}(4p^6)$ and the result was compared with the experimental total single ionization cross-section σ^+_{tot} [12] (see figure 4).

As can be seen, there is a good agreement in behaviors of the sum $\sigma_{dir}(5s^2) + \sigma_{EA}(4p^6)$ and the experimental σ^+_{tot} ionization cross-section [12] over the entire range of impact energies under consideration. This suggests that processes of the direct ionization of the $5s^2$ shell and the excitation-autoionization of the $4p^6$ shell adequately describe the single ionization of Sr atoms. From the comparison of the cross-sections at 24.5 eV impact energy one may conclude also that the $4p^6$ EA process (1)–(2) contributes up to 25% to the total single ionization cross-section of Sr atoms. Now, knowing the relative (25%) and absolute (2.5×10^{-16}cm^2) values of the EA cross-section and using a simple proportion we can estimate the upper limit for the 'real' value of the total single ionization cross-section σ^+_{tot}. In this case it should not exceed 10×10^{-16}cm^2. As can be seen from figure 3, the experimental data [14] are closest to this value.

4. Summary

In this paper, we present the $4p^6$ excitation-autoionization cross-section of Sr atoms obtained by accurate measuring the intensity of ejected-electron spectra arising from the decay of the $4p^5 n_1 l_1 n_2 l_2 n_3 l_3$ autoionizing states. The cross section reaches its maximum value $(2.5 \pm 0.8) \times 10^{-16}$ cm^2 at 24.5 eV impact energy, which indicates a strong resonance excitation of autoionizing states in configurations $4p^5 4d 5s^2$, $4p^5 4d^2 nl$ and $4p^5 4d 5s nl$. At high impact energies, the shape and magnitude of the cross-section are determined by the contribution of dipole-allowed autoionizing states belonging to the $4p^5 4d 5s^2$ and $4p^5 4d^2 5s$ configurations.

An analysis of the measured excitation-autoionization cross-section and the calculated single ionization cross-section

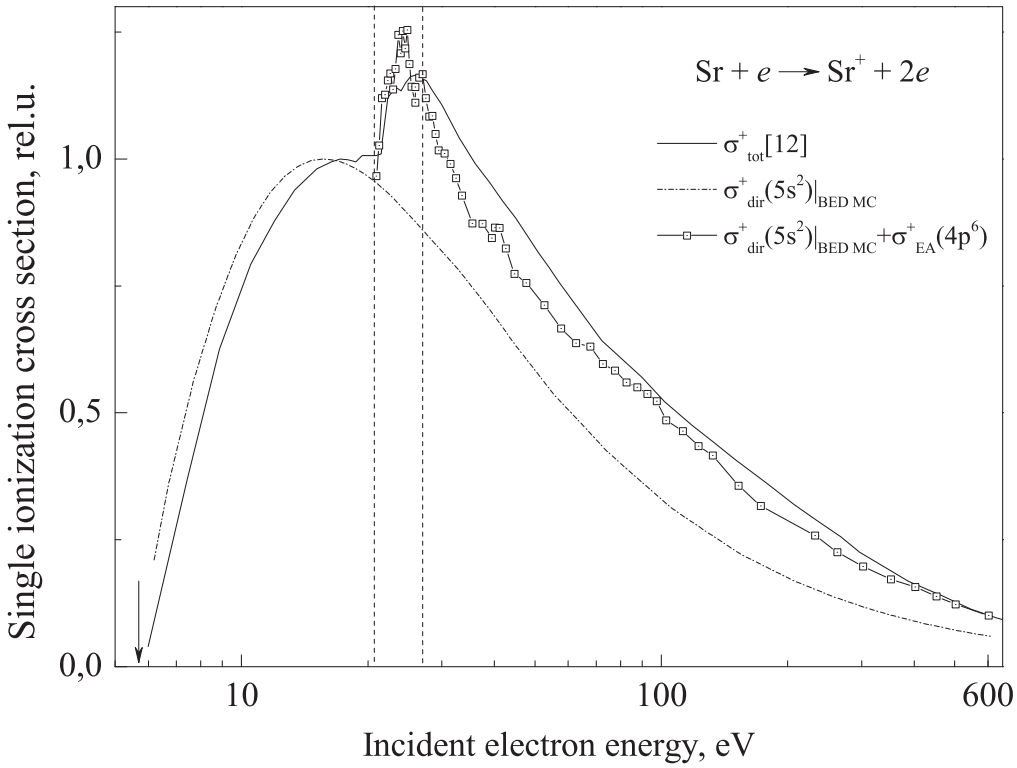

Figure 4. Strontium total single ionization cross-section σ^{+}_{tot} [12], the present BED MC single ionization cross-section $\sigma^{+}_{dir}(5s^2)$ and the sum $\sigma^{+}_{dir}(5s^2) + \sigma^{+}_{EA}(4p^6)$.

together with other available theoretical and experimental data showed that (i) direct ionization of the $5s^2$ shell and excitation-autoionization of the $4p^6$ shell adequately describe the single ionization of Sr atoms; (ii) $4p^6$ excitation-autoionization is the main indirect ionization process which contributes up to 25% to the total single ionization cross-section of Sr atoms by electron impact.

Acknowledgments

The calculated data presented in this pape4r were obtained by A V Kupliauskienė (1949–2018) within the framework of the Scientific Cooperation Agreement between the Institute of Electron Physics NASU and the Vilnius University.

This work was funded by the National Academy of Sciences of Ukraine through Projects Nos. 0112U002079, 0117U003239 and by the Ministry of Education and Science of Ukraine under Project No. 0118U000173.

ORCID iDs

O Borovik https://orcid.org/0000-0002-3111-2932

References

[1] Killiana T C, Pattard T, Pohl T and Rost J M 2007 *Phys. Rep.* **449** 77
[2] Calegari F, Sansone G, Stagira S, Vozzi C and Nisoli M 2016 *J. Phys. B: At. Mol. Opt. Phys.* **49** 062001
[3] Courtillot I, Quessada-Vial A, Brusch A, Kolker D, Rovera G D and Lemonde P 2005 *Eur. Phys. J.* D **33** 161
[4] Lemonde P 2009 *Eur. Phys. J. Special Topics* **172** 81
[5] Gorshkov A V, Rey A M, Daley A J, Boyd M M, Ye J, Zoller P and Lukin M D 2009 *Phys. Rev. Lett.* **102** 110503
[6] Jebahi S, Oudadesse H, el Feki H, Rebai T, Keskes H, Pellen P and el Feki A 2012 *J. Appl. Biomed.* **10** 195
[7] Adams C S, Pritchard J D and Shaffer J P 2020 *J. Phys. B: At. Mol. Opt. Phys.* **53** 012001
[8] Kramida A, Ralchenko Y, Reader J and NIST ASD Team 2018 NIST Atomic Spectra Database (ver. 5.6.1), [Online]. Available: https://physics.nist.gov/asd [2020, February 18]. National Institute of Standards and Technology, Gaithersburg, MD. (https://doi.org/10.18434/T4W30F)
[9] Starodub V P, Aleksakhin I S, Garga I I and Zapesochnyi I P 1973 *Opt. Spektrosc.* **35** 603
[10] Chen S T, Leep D and Gallagher A 1976 *Phys. Rev.* A **13** 947
[11] Ziesel J P 1967 *J. Chim. phys.* **64** 695
[12] Okudaira S 1970 *J. Phys. Soc. Jap.* **29** 409
[13] Okuno Y 1971 *J. Phys. Soc. Jap.* **31** 1189
[14] Veinshtein L A, Ochkur V I, Rakhovskii V I and Stepanov A M 1972 *Sov. Phys. -JETP* **34** 271
[15] Hudson R D, Carter V L and Young P A 1969 *Phys. Rev.* **180** 77
[16] Newsom G H, Connor S and Learner R C M 1973 *J. Phys. B: At. Mol. Phys.* **6** 2162
[17] Mansfield M W D and Connerade J P 1975 *Proc. R. Soc. Lond.* A **342** 421
[18] Mansfield M W D and Newsom G H 1981 *Proc. R. Soc. Lond.* A **377** 431
[19] Connerade J P, Baig M A and Sweeney M 1990 *J. Phys. B: At. Mol. Opt. Phys.* **23** 713
[20] Schmitz W, Breuckmann B and Mehlhorn W 1976 *J. Phys. B: At. Mol. Phys.* **9** L493

[21] White M D, Rassi D and Ross K J 1979 *J. Phys. B: At. Mol. Phys.* **12** 315
[22] Borovik A A, Aleksakhin I S, Bratsev V F and Kuplyauskene A V 1982 *Opt. Spectrosk.* **53** 976 (in Russian)
[23] Kazakov S M and Khristoforov O V 1985 *Sov. Phys. - JETP* **61** 656
[24] Borovik A, Vakula V and Kupliauskiene A 2007 *Lith. J. Phys.* **47** 129
[25] Kupliauskienė A, Kerevičius G, Borovik V, Shafranyosh I and Borovik A 2017 *J. Phys. B: At. Mol. Opt. Phys.* **50** 225201
[26] Jacobs V L 1995 *J. Quant. Spectrosc. Radiat. Transfer* **54** 195
[27] Christophorou L G and Olthoff J K 2001 *Advances in Atomic, Molecular, and Optical Physics* **44** 59
[28] Lepp S, Stancil P C and Dalgarno A 2002 *J. Phys. B: At. Mol. Opt. Phys.* **35** R57
[29] Borovik A, Kupliauskiene A and Zatsarinny O 2013 *J. Phys. B: At. Mol. Opt. Phys.* **46** 215201
[30] Borovik V, Roman V, Kupliauskiene A, Shafranyosh I and Borovik O 2019 *Eur. Phys. J.* D **73** 43
[31] Roy B N and Rai D K 1983 *J. Phys. B: At. Mol. Phys.* **16** 46
[32] Mitnik D, Mandelbaum P, Schwob J L, Bar-Shalom A, Oreg J and Goldstein W H 1994 *Phys. Rev.* A **50** 4911
[33] Berezhko E G and Kabachnik N M 1977 *J. Phys. B: At. Mol. Phys.* **10** 2467
[34] Borovik A A, Grum-Grzhimailo A N, Bartschat K and Zatsarinny O I 2005 *J. Phys. B: At. Mol. Opt. Phys.* **38** 1081
[35] Hrytsko V, Kerevičius G, Kupliauskienė A and Borovik A 2016 *J. Phys. B: At. Mol. Opt. Phys* **49** 145201
[36] Borovik A A 2008 *Ukr. J. Phys.* **53** 1021 2071-0194
[37] Kim Y K and Rudd M E 1994 *Phys. Rev.* A **50** 3954
[38] Lotz W 1970 *Z. Physik* **232** 101
[39] Gu M F 2008 *Can. J. Phys.* **86** 675
[40] Roman V, Kupliauskiene A and Borovik A 2015 *J. Phys. B: At. Mol. Opt. Phys.* **48** 205204
[41] Nagata T *et al* 1986 *J. Phys. B: At. Mol. Phys.* **19** 1281
[42] Hotop H and Mahr D 1975 *J. Phys. B: At. Mol. Phys.* **8** L301
[43] Peart B and Dolder K 1975 *J. Phys. B: At. Mol. Phys.* **8** 56